

SUPPLEMENTARY MATERIALS FOR

Hyman DM, Smyth LM, et al. AKT inhibition in solid tumors with AKT1 mutations.

Supplemental Methods

Study participants and genomic sequencing

Tumor and blood specimens from the 58 study participants were profiled by a combination of whole-exome and deep targeted sequencing as well as with digital droplet PCR (ddPCR). For the 23 patients for whom we possessed matched normal specimens, their samples underwent MSK-IMPACT and WES sequencing, for those lacking a matched normal Foundation Medicine sequencing was used. The platforms utilized per patient are specified in **Table S1**.

Plasma cfDNA extraction and analyses

Whole blood was collected for MSKCC patients in 10-ml Cell-Free DNA BCT tubes (STRECK) was centrifuged in two steps to separate plasma from cells. Initially, whole blood was centrifuged at 800 X g for 10 min (ambient temperature). Plasma was then separated from red blood cells. In the second phase, separated plasma was further centrifuged in a high-speed micro-centrifuge at 18,000 X g for 10 min (ambient temperature). Cell-free plasma was aliquoted and frozen at minus 80°C until extraction. Extraction of cfDNA was performed using a fully automated QIAGEN platform, QIASymphony SP, and QIASymphony DSP Virus/Pathogen Midi Kit (catalog #937055). This bead-based custom protocol was optimized to work with 3ml of plasma as starting material. The extraction process includes lysis, binding, wash, and elution steps. The final product is a 60µl elution of cfDNA with an average size ~170-200 bp. Quality and quantity of cfDNA was evaluated with automated electrophoresis using either TapeStation with High Sensitivity D1000 ScreenTape and Reagents (Agilent Technologies) or Fragment Analyzer with High Sensitivity genomic DNA Analysis Kit (Advanced Analytical). Plasma extraction for non-MSK patients was as follows. In total, 10 or 20mL of whole blood were collected at individual local study sites into venous blood collection tubes containing EDTA as anti-coagulant. Within 1 hour, plasma was processed by centrifugation at approximately 2000G for 10mins using a pre-chilled centrifuge set to 4°C. Plasma was then transferred to a 15mL Falcon tube, centrifuged as above at approximately 2000G for 10mins, aliquoted, and frozen at minus 80°C until extraction

Digital droplet PCR profiling of tumor-derived cell-free DNA

The AKT E17K mutation was detected utilizing a pre-validated PrimePCR ddPCR mutation assay was used (Biorad, assay ID dHsaCP2000032). ESR1 mutations were detected via custom assays designed and ordered through through Biorad and were as follows:

- ESR1 D538G: forward primer 5' TACAGCATGAAGTGCAAG 3'; reverse primer: 5' TGGGCGTCCAGCA 3'; wildtype probe: 5' CCCCTCTATGACCTGCT 3'-HEX_lowaBlack; mutation-specific probe: 5' CTCTATGgCCTGCTGC 3'- FAM_lowaBlack.
- ESR1 Y537N: forward primer 5' TACAGTAACAAAGGCATGG 3'; reverse primer: 5' CGTCCAGCATCTCCAG 3'; wildtype probe: 5' CCCCTCTATGACCTGCT 3'-HEX_lowaBlack; mutation-specific probe: 5' CCCCTCAATGACCTGC 3'-FAM_lowaBlack.

- ESR1 Y537C: forward primer 5' TACAGTAACAAAGGCATGG 3'; reverse primer: 5' CGTCCAGCATCTCCAG 3'; wildtype probe: 5' CCCCTCTATGACCTGCT 3'-HEX_lowaBlack; mutation-specific probe: 5' TGCCCCTCTGTGACC 3'-FAM_lowaBlack.
- ESR1 Y537S: forward primer 5' GTACAGCATGAAGTGCAA 3'; reverse primer: 5' GGGCGTCCAGCATC 3'; wildtype probe: 5' AGCAGGTCAAGAGGGG 3'-HEX_lowaBlack; mutation-specific probe: 5' AGCAGGTCAgAGAGGG 3'-FAM_lowaBlack.

Cycling conditions were tested to ensure optimal annealing/extension temperature as well as optimal separation of positive from empty droplets. All reactions were performed on a QX200 ddPCR system (Biorad) for which we load 9ul cfDNA per ddPCR reaction or for gDNA, first dilute to 1ng/ul. Each sample was evaluated in technical duplicates. Each PCR reaction contains primers, probes, DNA, and digital PCR Supermix for probes (no dUTP). Reactions were partitioned into a median of ~16,000 droplets per well using the QX200 droplet generator. Emulsified PCRs were run on a 96-well thermal cycler using cycling conditions identified during the optimization step (95°C 10'; 40 cycles of 94°C 30'' 55°C 1', 98°C 10', 4°C hold). In every run, wells of water, gDNA, and a mutation-positive control are included (for manual processing: 1 of each, for robotic processing, two of each). Plates were read and analyzed with the QuantaSoft software to assess the number of droplets positive for mutant DNA, wild-type DNA, both, or neither. The assay threshold sensitivity was set at 1 mutant droplets.

Genomic sequencing data and analysis

Sequencing of baseline pre-treatment specimens was performed with one of several possible platforms. In 42 of 52 patients, exon-capture and deep targeted sequencing was performed utilizing the MSK-IMPACT assay on tumor and matched normal tissues (either a 341-gene or 410-gene version of the assay, n=10 and 11 respectively) or cfDNA (n=4); Foundation Medicine on tumor tissue (n=17). Additional whole-exome sequencing (WES) was performed from remaining library of 19 patients who previously underwent MSK-IMPACT sequencing. MSK-IMPACT, Foundation Medicine, and WES data were analyzed as previously described¹⁻³. All mutation calls across platforms were post-processed and annotated to ensure cross-comparison. Briefly, mutations were annotated with VEP (version 85) and common variants identified by the Exome Aggregation Consortium (ExAC)⁴ as having a minor allele frequency greater than 0.0004 in any subpopulation were excluded as presumed germline (<https://github.com/mskcc/vcf2maf>). Furthermore, only mutations with a variant allele frequency greater than 5% were considered (as per New York State clinical testing standards for IMPACT sequencing), with the exception of known hotspot mutations that were reported regardless of allele frequency in the sequenced specimen. Hotspot mutations were those identified by an adaptation of methodologies described previously⁵ applied to a cohort of ~24592 sequenced human cancers (Chang MT et al. *submitted*). Mutations with low numbers of supporting reads or those called in repeat regions were also flagged for manual inspection. Where available, ddPCR results on cfDNA specimens were utilized to orthogonally confirm (or identify at higher sensitivity than sequencing data) the presence of individual mutations (AKT1 E17K and ESR1 Y537C, Y537N, Y537S, and D538G). As we do not observe mutation-positive droplets in either water and gDNA negative control wells (considered run failure and is repeated), a single mutant droplet from ddPCR was considered sufficient to identify the presence of a mutation. For individual somatic mutations in genes of interest in this analysis that are not recurrently mutated hotspots, we assessed whether they were likely functional by exploring their paralogy with

mutated members of highly related protein families as well as their position in the three dimensional structure of the folded cognate protein. Notable mutations were annotated as such throughout the text and figures or were otherwise assumed to be mutations of unknown significance.

Copy number and allelic imbalance

In patients for which either MSK-IMPACT or WES sequencing existed of tumor and matched normal specimens, total, allele-specific, and integer copy number genome-wide was generated using joint segmentation of read counts spanning polymorphic SNPS with FACETS⁶ (<https://github.com/mskcc/facets>). FACETS inference of tumor purity, ploidy, and clonal heterogeneity corrected integer copy number calls were then used to determine the presence and type of mutant allelic imbalance. *AKT1* allelic imbalance was defined as unequal copy number of mutant to WT alleles for individual somatic mutations in each patient. For the purposes of this analysis, heterozygous loss of the wildtype allele, focal amplification of the mutant allele, and copy-neutral loss-of-heterozygosity (CN-LOH) were all considered examples of allelic imbalance. For patients with Foundation Medicine sequencing only, and therefore, lacking a sequenced matched normal sample; we determined the distribution of mutant allele frequency from all mutations after common variant filtering and excluding *AKT1* E17K. We then used a modified z-score using the median and median absolute deviation (MAD) to determine whether the allelic frequency of *AKT1* E17K deviated significantly from the median mutant allele frequency of the sample overall. In the absence of a focal copy number alteration called by the standard Foundation Medicine analysis pipeline, we inferred that CN-LOH was present if the *AKT1* E17K allele frequency was significantly higher (z-mad, nominal p-value < 0.05) than all other mutations present, with the assumption that most somatic mutations in patients enrolled here were clonal heterozygous corrected for clear biallelic loss of tumor suppressor gene mutations (for instance, *TP53*). However, due to the FMI pipeline only calling copy number increases for five copies or more, the precise mechanism of allelic imbalance, be it loss of wildtype and/or broad single-copy genomic gains, cannot be inferred and they are labeled ambiguous. For patients for which only MSK-IMPACT sequencing of baseline cfDNA was available, allelic imbalance was inferred in a manner similar to Foundation Medicine sequenced-patients. However, we further confirmed the presence of allelic imbalance in the cfDNA samples by plotted the minor (B) allele frequencies after genotyping all polymorphic SNPs present in the design of the MSK-IMPACT assay with sufficient coverage.

Clonality analysis

The clonality of all somatic mutations was inferred in patients with tumor tissue and matched normal sequencing data from either MSK-IMPACT or WES. For each somatic mutation, cancer cell fractions (CCFs) were estimated as previously described⁷ and for those mutations in regions of genomic gains, two CCFs were calculated, assuming the minimum and maximum possible number of copies. The probability of a mutation's CCF was calculated with a binomial distribution using maximum likelihood (ML) estimation, which we normalize to produce posterior probabilities. Confidence intervals (CI) for the CCF are calculated as the full-width-at-half-maximum of the ML value. Mutations were defined clonal if the upper confidence interval overlapped 0.85; otherwise they were defined as subclonal.

Mutant allele imbalance analysis public genomic data

Whole-exome sequencing data from tumor and matched normal sample pairs were downloaded from CGHub as BAM files for the following tumor types: breast carcinoma (BRCA; n=940), uterine carcinoma (UCEC; n=245), lung adenocarcinoma (LUAD; n=495), cutaneous melanoma (SKCM; n=367), colorectal carcinoma (COADREAD; n=491), and stomach adenocarcinoma (STAD; n=247). As with patients studied here, total, allele-specific, and integer copy number was inferred using FACETS via the procedure described above. Publicly available mutation calls for these cohorts were utilized and samples were split into two groups, those harboring a hotspot mutation in the genes of interest (*AKT1*, *EGFR*, *BRAF*, *ERBB2*, and *PIK3CA*) and those without. For each combination of gene and tumor type, the number of samples (*N*) harboring LOH spanning the gene of interest for those samples harboring hotspots was determined. Based on this number, those samples without hotspot mutations in the gene of interest were randomly sampled with replacement *N* times and the number of samples with LOH spanning the same locus but in samples lacking the mutation was determined. This was repeated (for each gene and tumor type combination) 100,000 times to produce an empirical null distribution of genomic LOH at the locus. The rank of the observed data was used to determine whether LOH was significantly enriched in those samples harboring hotspots in the gene of interest compared to this background distribution and significant associations were those of simulated p-value < 0.05 after correction for multiple testing.

Statistical analysis and figures

Cox proportional hazards analysis and Kaplan-Meier plots were performed and generated using the R survival package. Patients who progressed or died after two or more missed visits were censored at the time of the latest evaluable RECIST 1.1 assessment prior to the two missed visits. Individual associations among genomic changes and response were assessed by either Fisher Exact or chi-squared tests (where appropriate) and nominal p-values are specified. Additional figures were generated using R ggplot2 and similar.

Supplementary Results

Persistent clearance of circulating *AKT1* E17K (>21 days) correlated with objective response, with all five patients meeting this criteria achieving partial responses lasting ≥18 weeks (p=0.025).

Supplementary Figures

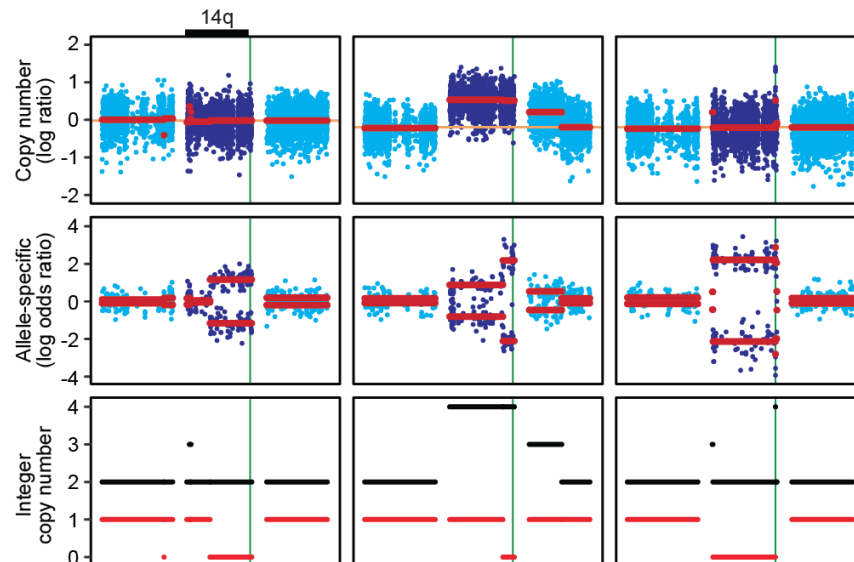


Figure S1: Mutant allele imbalance affect the *AKT1* locus. Shown are three representative patients with different genetic configurations of the *AKT1* E17K mutation inferred from total (top), allele-specific (middle), and integer (bottom) DNA copy number analysis. Chromosomes 13-15 are shown and the *AKT1* locus on 14q is identified (green line) and segmentation of copy number loci is shown in red (top and middle). The first tumor (leftmost column) possesses 14q CN-LOH duplicating *AKT1* E17K and eliminating the WT allele (top, middle rows) producing two mutant and zero wildtype copies of *AKT1* (bottom row). The second tumor (middle column) had a focal CN-LOH spanning *AKT1* followed by a two-copy gain of chromosome 14 producing four mutant and zero wildtype copies of *AKT1*. The final tumor (rightmost column) possesses whole chromosome 14 CN-LOH duplicating the *AKT1* E17K allele followed by focal amplification again producing four mutant and zero wildtype copies of *AKT1*.

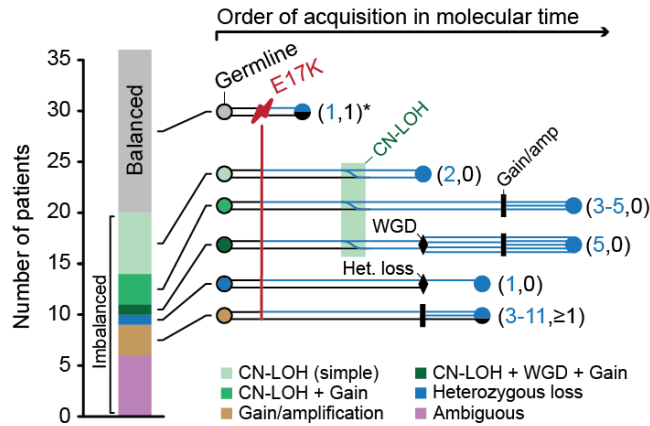


Figure S2: Genomic configuration of AKT mutations. Fifty-seven percent of patients possessed AKT1 E17K allelic imbalance, the majority of which was due to loss of wild-type AKT1 via CN-LOH that duplicated the mutant allele, while a subset of patients harbored a more complex pattern of additional lesions targeting the E17K mutant allele (right). At left is a schematic representation of the order of acquisition of lesions in molecular time targeting AKT1 E17K that were inferred from tumor sequencing. Lines indicate the count of wildtype (black) and mutant (blue) copies of AKT1 with genomic events annotated. Numbers in parentheses are the final count of wildtype and mutant copies in the tumor. Amplification refers to a focal event of greater than 3 additional copies while genomic gain refers to broad or chromosome arm-length events of 1 or 2 additional copies.

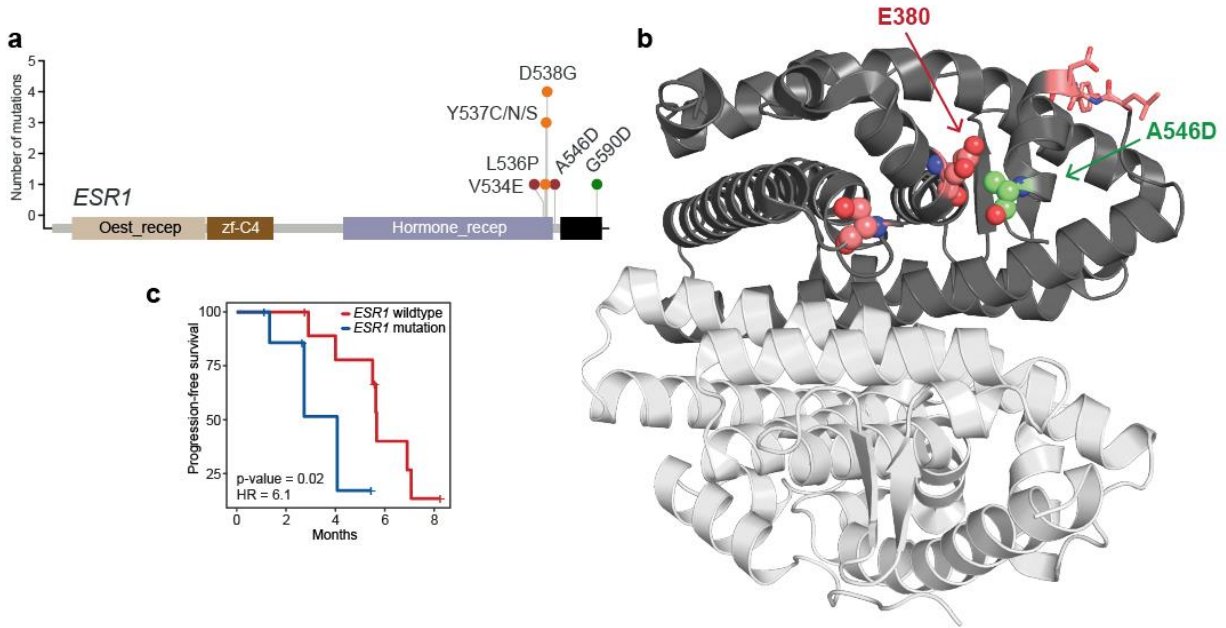


Figure S3: ESR1 mutations in study participants. **a.** Schematic of ESR1 is shown with the position and frequency of somatic mutations detected in this patient cohort. **b.** The position and physical adjacency of candidate mutations A546D with known ligand-binding domain hotspot mutations in the three dimensional structure of ESR1. **c)** ER+ breast cancer patients with ESR1-mutant tumors had shorter PFS compared to those that lacked ESR1 mutations (HR=6.1, $p=0.02$).

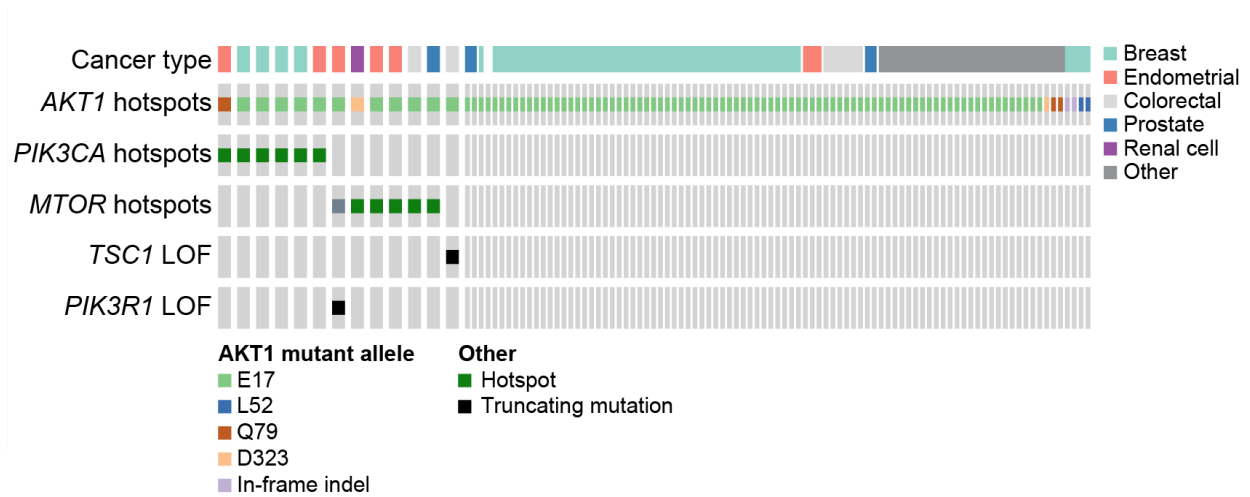


Figure S4: Co-occurring PI3K/mTOR mutations in AKT1-mutant cancers. Pan-cancer analysis of 10,336 prospectively sequenced human tumor specimens (Zehir A, et al. *submitted*) indicates that 12% of cancers with one of several recurrent activating *AKT1* mutations also possess activating mutations in other effectors of PI3K/mTOR signaling.

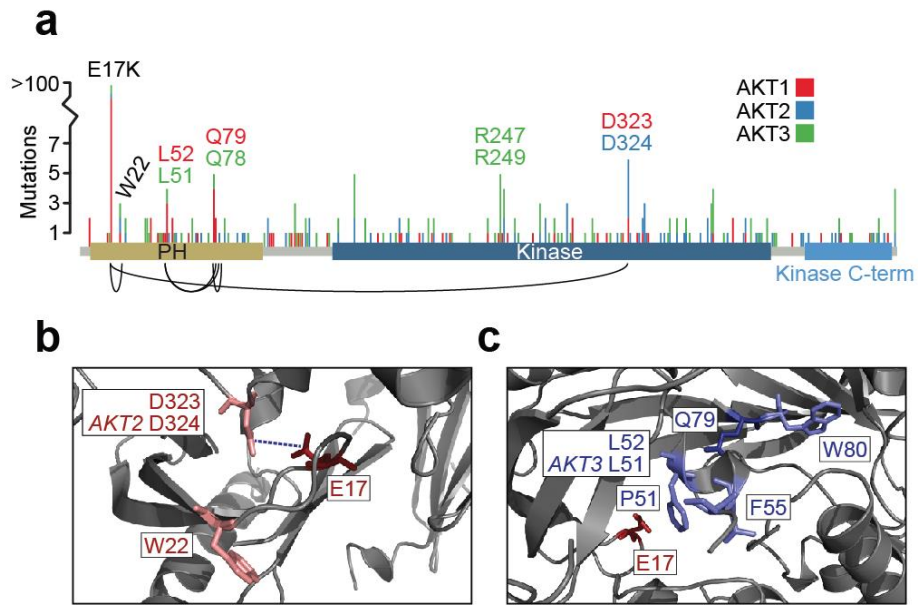


Figure S5: Candidate non-AKT1 E17K activating mutations of AKT isoforms. a) Somatic mutations in paralogous residues of *AKT1*, *AKT2*, and *AKT3* jointly aligned. Arcs reflect physical proximity 3D. **b-c)** Clusters of physically adjacent mutations in protein structure.

Supplementary Tables

Table S1: Patient level clinical data.

Subject	Cohort	Therapy	Best % change ^[b]	AKT1	Best objective response	Treatment duration	PFS (adjusted)	Censored (adjusted)	PFS (unadjusted)	Censored (unadjusted)	Data
B.6	Breast	Mono	-11.6	E17K	SD	148	170	No	170	No	FMI
B.14	Breast	Mono	-25	E17K	SD	22	82	Yes	82	Yes	FMI
B.8	Breast	Mono	-13.3	E17K	SD	186	167	Yes	167	Yes	FMI
B.3	Breast	Mono	14	E17K	NE	39	33	Yes	379	No	FMI
G.23	Gyn	Mono	28.8	E17K	PD	39	39	No	39	No	FMI
G.35	Gyn	Mono	-80 ^[a]	E17K	PR	144	253	Yes	253	Yes	FMI
G.26	Gyn	Mono	-1.6	E17K	SD	291	372	No	372	No	FMI
G.22	Gyn	Mono	.	E17K	PD	47	40	No	40	No	FMI
O.42	Other	Mono	-9.4	E17K	SD	82	36	No	36	No	FMI
O.47	Other	Mono	-25.7	E17K	SD	212	337	Yes	337	Yes	FMI
O.36	Other	Mono	29.9	E17K	PD	39	43	No	43	No	FMI
O.49	Other	Mono	-33.3	E17K	uPR	102	64	Yes	64	Yes	FMI
O.39	Other	Mono	10	E17K	SD	18	39	Yes	200	No	FMI
O.51	Other	Mono	-46.7	E17K	uPR	70	130	No	130	No	FMI
O.52	Other	Mono	-79.2	E17K	PR	81	126	No	126	No	FMI
O.44	Other	Mono	-11.3	E17K	SD	81	80	No	80	No	FMI
O.40	Other	Mono	0	E17K	SD	174	191	Yes	191	Yes	FMI
B.5	Breast	Mono	0	E17K	SD	84	82	No	82	No	MSK-cf
B.2	Breast	Mono	17.4	E17K	PD	39	40	No	40	No	MSK-cf
O.46	Other	Mono	-23.3	E17K	SD	46	64	No	64	No	MSK-cf
O.41	Other	Mono	-1.5	E17K	SD	82	78	No	78	No	MSK-cf
B.16	Breast	Mono	-33.3 ^[a]	E17K	PR	207	163	Yes	163	Yes	MSK-T
B.18	Breast	Mono	-45.7	E17K	PR	207	212	No	212	No	MSK-T
B.15	Breast	Mono	-30.8	E17K	uPR	169	165	No	165	No	MSK-T
B.12	Breast	Mono	-20	E17K	SD	86	79	Yes	79	Yes	MSK-T
B.19	Breast	Mono	-65.1	E17K	PR	212	207	No	207	No	MSK-T
B.11	Breast	Mono	-18.2	E17K	SD	94	87	No	87	No	MSK-T
B.20	Breast	Mono	-70.8	E17K	uPR	64	82	No	82	No	MSK-T
B.9	Breast	Mono	-15.2	E17K	SD	130	122	No	122	No	MSK-T
B.7	Breast	Mono	-12.2	E17K	SD	137	120	No	120	No	MSK-T
B.17	Breast	Mono	-44.2	E17K	PR	248	247	Yes	247	Yes	MSK-T
B.4	Breast	Mono	4.3	E17K	SD	166	169	No	169	No	MSK-T
B.13	Breast	Mono	-21.6	E17K	SD	122	122	No	122	No	MSK-T
G.34	Gyn	Mono	-50 ^[a]	E17K	PR	333	339	Yes	339	Yes	MSK-T
G.28	Gyn	Mono	-19	E17K	SD	254	250	No	250	No	MSK-T
G.25	Gyn	Mono	0	E17K	SD	86	117	No	117	No	MSK-T
G.32	Gyn	Mono	-24.2	E17K	SD	253	248	No	248	No	MSK-T
G.33	Gyn	Mono	-30	E17K	PR	245	247	No	247	No	MSK-T
G.24	Gyn	Mono	17.5	E17K	SD	54	78	No	78	No	MSK-T
O.48	Other	Mono	-30.8	E17K	SD	134	130	No	130	No	MSK-T
O.38	Other	Mono	13.6	E17K	SD	81	78	No	78	No	MSK-T
O.50	Other	Mono	-38.9	E17K	PR	381	385	No	385	No	MSK-T
B.1	Breast	Mono	.	E17K	PD	24	59	No	59	No	-
B.10	Breast	Mono	-16.3	E17K	SD	217	238	Yes	636	No	-
G.31	Gyn	Mono	-22.2	E17K	SD	22	131	Yes	399	No	-
G.27	Gyn	Mono	-3.7	E17K	SD	29	52	Yes	52	Yes	-
G.30	Gyn	Mono	-21.6	E17K	SD	184	197	No	197	No	-
G.29	Gyn	Mono	-19.3	E17K	SD	175	178	No	178	No	-
G.21	Gyn	Mono	.	E17K	PD	18	45	No	45	No	-
O.45	Other	Mono	-19.4 ^[a]	E17K	SD	32	116	Yes	116	Yes	-
O.43	Other	Mono	-9.6	E17K	SD	170	172	Yes	302	No	-

O.37	Other	Mono	17.2	E17K PD	10	10	No	10	No	-
G.56	Gyn	Mono	0	T34N PD	40	43	No	43	No	FMI
G.58	Gyn	Mono	-25 ^[a]	Q79K SD	424	380	Yes	380	Yes	FMI
O.55	Other	Mono	4.8	V201A NE	10	22	Yes	22	Yes	FMI
O.57	Other	Mono	-18.2	Q79K PD	38	37	No	37	No	MSK-T
O.54	Other	Mono	28.6	F35L PD	1	22	No	22	No	-
G.53	Gyn	Mono	.	N.D. PD	1	11	No	11	No	-
B.15	Breast	Combo	-23	E17K PD	39	36	NA	36	NA	See above
B.12	Breast	Combo	0	E17K SD	80	84	NA	84	NA	See above
B.19	Breast	Combo	.	E17K NE	4	1	NA	1	NA	See above
B.9	Breast	Combo	-22.2	E17K SD	245	244	NA	244	NA	See above
B.7	Breast	Combo	8.3	E17K NE	29	29	NA	29	NA	See above
G.28	Gyn	Combo	-2	E17K PD	38	38	NA	38	NA	See above

[a] Ongoing monotherapy. [b] Best percentage change in target lesions. MSK, MSK-IMPACT sequencing of tissue (T) or cfDNA (cf). FMI, Foundation Medicine. PFS, progression-free survival; PR, partial response; uPR, unconfirmed partial response; SD, stable disease; NE, not evaluable PD, progressive disease; N.D. Not detected; Gyn, Gynaecological

Table S2: Drug-related serious adverse events. All patients in the safety analysis received at least one dose of AZD5363 and events are listed as assessed by the investigator. SAE, serious adverse event.

Any SAE	Total (N=58)
Number of patients (%)	9 (15.5)
Number of events	17
SAE by preferred term, n (%)	
Diarrhea	3 (5.2)
Acute kidney injury	2 (3.4)
Confusional state	2 (3.4)
Dehydration	2 (3.4)
Hypersensitivity	2 (3.4)
Acute hepatic failure	1 (1.7)
Cerebrovascular accident	1 (1.7)
Electrolyte imbalance	1 (1.7)
Hyperglycaemia	1 (1.7)
Nausea	1 (1.7)
Renal failure	1 (1.7)

Table S3: Somatic mutations. All somatic mutations identified at baseline from patients with either tissue or cfDNA sequencing, as indicated.

Subject	Chr	Gene	Start Position	End Position	Ref. Allele	Alt. Allele	Tumor		Normal		Data source
							Depth	Count	Depth	Count	
O.46	14	<i>AKT1</i>	105246551	105246551	C	T	259	73	421	0	MSK-cf
O.46	6	<i>ARID1B</i>	157099426	157099427	A	ACAGCAG	151	35	375	0	MSK-cf
O.46	17	<i>TP53</i>	7578191	7578191	A	T	400	161	569	0	MSK-cf
O.46	9	<i>TSC1</i>	135771966	135771966	G	A	118	58	284	0	MSK-cf
B.5	14	<i>AKT1</i>	105246551	105246551	C	T	217	36	326	0	MSK-cf
B.5	11	<i>ATM</i>	108192065	108192065	G	C	140	41	444	0	MSK-cf
B.2	X	<i>ARAF</i>	47424198	47424198	G	A	555	85	403	0	MSK-cf
B.2	6	<i>ESR1</i>	152419926	152419926	A	G	231	73	408	0	MSK-cf
B.2	10	<i>GATA3</i>	8115952	8115953	A	AC	160	15	283	0	MSK-cf
O.41	14	<i>AKT1</i>	105246551	105246551	C	T	139	14	421	0	MSK-cf
O.41	X	<i>RBM10</i>	47038741	47038741	G	A	170	71	242	0	MSK-cf
O.41	18	<i>SMAD4</i>	48604788	48604788	A	G	168	8	325	0	MSK-cf
B.16	16	<i>CTCF</i>	67645922	67645922	C	T	581	368	486	0	MSK-T
B.16	3	<i>PIK3CA</i>	178936091	178936091	G	A	410	198	163	0	MSK-T
B.16	5	<i>MAP3K1</i>	56155725	56155726	AG	-	760	271	262	0	MSK-T
B.16	5	<i>MAP3K1</i>	56160564	56160567	CAGA	-	637	216	212	0	MSK-T
B.16	6	<i>ESR1</i>	152419914	152419914	T	A	730	151	238	0	MSK-T
B.16	6	<i>ESR1</i>	152419950	152419950	C	A	742	302	273	0	MSK-T
B.16	X	<i>BCOR</i>	39913284	39913285	-	ATCATCT G	534	147	364	0	MSK-T
B.15	15	<i>IGF1R</i>	99465600	99465600	G	A	272	97	239	0	MSK-T
B.15	18	<i>SMAD4</i>	48591924	48591924	T	C	210	105	356	0	MSK-T
B.15	9	<i>NOTCH1</i>	139413225	139413225	C	G	283	76	393	0	MSK-T
G.34	1	<i>MTOR</i>	11188164	11188164	G	A	646	150	340	0	MSK-T
G.34	16	<i>CREBBP</i>	3900884	3900884	G	A	976	261	653	0	MSK-T
G.34	3	<i>CTNNB1</i>	41266104	41266104	G	T	647	163	517	0	MSK-T
G.34	6	<i>ESR1</i>	152419920	152419920	T	C	724	195	672	0	MSK-T
B.19	13	<i>BRCA2</i>	32912298	32912298	T	A	553	288	635	0	MSK-T
B.19	17	<i>TP53</i>	7577085	7577085	C	T	480	314	486	0	MSK-T
B.19	17	<i>TP53</i>	7577127	7577127	C	G	526	361	511	0	MSK-T
G.28	17	<i>SOX9</i>	70117769	70117807	GGTGC TCAAAG GCTAC GACTG GACGC TGGTG CCCAT GCC	-	1342	73	567	0	MSK-T
G.28	21	<i>U2AF1</i>	44524456	44524456	G	A	1060	414	386	0	MSK-T
G.28	3	<i>CTNNB1</i>	41266097	41266097	G	T	1105	427	624	0	MSK-T
G.25	3	<i>CTNNB1</i>	41266113	41266113	C	T	455	225	426	0	MSK-T
O.38	3	<i>SETD2</i>	47144879	47144879	C	T	792	108	475	0	MSK-T
B.20	10	<i>RET</i>	43604517	43604517	C	T	308	84	403	0	MSK-T
B.20	16	<i>AXIN1</i>	348025	348025	G	C	208	66	354	0	MSK-T
B.20	16	<i>CDH1</i>	68856084	68856085	-	A	248	87	469	0	MSK-T
B.20	6	<i>IRF4</i>	398843	398843	G	C	338	77	396	0	MSK-T

B.9	19	KEAP1	10610249	10610250	-	GGA	561	179	579	0	MSK-T
B.7	10	GATA3	8111433	8111434	CA	-	701	97	274	0	MSK-T
B.7	16	CBFB	67070594	67070594	G	A	655	86	490	0	MSK-T
B.7	17	NF1	29654689	29654690	-	C	734	82	387	0	MSK-T
G.32	21	RUNX1	36171722	36171723	-	T	344	96	135	0	MSK-T
G.32	3	FOXL2	138665163	138665163	G	C	425	217	554	0	MSK-T
G.32	5	TERT	1295228	1295228	G	A	53	26	186	0	MSK-T
G.32	X	KDM5C	53241030	53241031	AG	-	777	223	429	0	MSK-T
G.33	17	NF1	29548886	29548886	C	T	629	138	233	0	MSK-T
G.33	4	FGFR3	1803568	1803568	C	G	398	17	188	0	MSK-T
G.33	4	TET2	106157758	106157758	G	A	847	174	277	0	MSK-T
G.33	5	FLT4	180038431	180038431	C	T	559	47	336	0	MSK-T
B.17	17	TP53	7577545	7577545	T	G	550	53	602	0	MSK-T
B.17	21	RUNX1	36164881	36164881	C	G	512	26	284	0	MSK-T
B.17	3	PIK3CA	178936095	178936095	A	C	315	59	307	0	MSK-T
G.24	1	ARID1A	27057781	27057781	C	T	820	275	671	0	MSK-T
G.24	3	CTNNB1	41266101	41266101	C	T	700	207	559	0	MSK-T
B.4	12	POLE	133263850	133263850	C	T	264	31	297	0	MSK-T
B.4	17	TP53	7577099	7577099	C	T	839	93	579	0	MSK-T
B.4	19	STK11	1220502	1220502	G	A	702	72	475	0	MSK-T
B.4	21	RUNX1	36259206	36259206	G	-	855	77	431	0	MSK-T
B.4	22	EP300	41545822	41545822	C	T	1179	122	599	0	MSK-T
B.4	9	FANCC	97933379	97933379	C	T	796	72	392	0	MSK-T
O.57	14	AKT1	105243048	105243048	G	T	1725	603	496	0	MSK-T
O.57	8	MYC	128752800	128752800	C	G	254	77	230	0	MSK-T
O.46	2	IDH1	209113112	209113112	C	T	170	31	183	1	MSK-cf
B.15	17	TP53	7578410	7578410	T	C	146	63	255	1	MSK-T
B.12	6	ESR1	152419923	152419923	A	C	579	182	351	1	MSK-T
B.19	16	CTCF	67645935	67645935	A	G	596	447	370	1	MSK-T
G.28	4	FAT1	187554954	187554955	-	T	1147	440	540	1	MSK-T
O.48	10	GATA3	8115750	8115750	C	T	748	342	620	1	MSK-T
O.38	3	RAF1	12641706	12641706	A	T	843	83	437	1	MSK-T
O.38	X	ATRX	76909634	76909634	T	C	1178	83	766	1	MSK-T
G.33	19	MAP2K2	4110623	4110623	G	A	752	175	299	1	MSK-T
B.17	16	CTCF	67644880	67644881	-	AGGT	733	107	621	1	MSK-T
B.15	10	GATA3	8111502	8111503	-	G	425	168	530	2	MSK-T
G.28	1	ARID1A	27087503	27087503	C	T	1086	438	620	2	MSK-T
B.11	1	SDHB	17350515	17350515	A	C	527	134	619	2	MSK-T
B.16	14	AKT1	105246551	105246551	C	T	665	365	207	1	MSK-T
B.15	14	AKT1	105246551	105246551	C	T	248	90	281	0	MSK-T
B.12	14	AKT1	105246551	105246551	C	T	721	567	320	0	MSK-T
G.34	14	AKT1	105246551	105246551	C	T	674	385	475	0	MSK-T
B.19	14	AKT1	105246551	105246551	C	T	853	436	237	0	MSK-T
G.28	14	AKT1	105246551	105246551	C	T	1685	1542	297	0	MSK-T
G.25	14	AKT1	105246551	105246551	C	T	1402	1295	368	0	MSK-T
B.11	14	AKT1	105246551	105246551	C	T	462	244	497	1	MSK-T
O.48	14	AKT1	105246551	105246551	C	T	527	312	263	0	MSK-T
O.38	14	AKT1	105246551	105246551	C	T	385	32	456	0	MSK-T
B.20	14	AKT1	105246551	105246551	C	T	209	108	294	0	MSK-T
B.9	14	AKT1	105246551	105246551	C	T	341	127	315	0	MSK-T
B.7	14	AKT1	105246551	105246551	C	T	413	109	285	0	MSK-T
G.32	14	AKT1	105246551	105246551	C	T	360	6	547	0	MSK-T
G.33	14	AKT1	105246551	105246551	C	T	507	325	260	1	MSK-T
B.17	14	AKT1	105246551	105246551	C	T	945	260	442	0	MSK-T

G.24	14	<i>AKT1</i>	105246551	105246551	C	T	518	375	312	0	MSK-T
B.4	14	<i>AKT1</i>	105246551	105246551	C	T	555	92	326	0	MSK-T
B.13	14	<i>AKT1</i>	105246551	105246551	C	T	100	36	677	0	MSK-T
O.50	14	<i>AKT1</i>	105246551	105246551	C	T	175	87	294	0	MSK-T
B.18	14	<i>AKT1</i>	105246551	105246551	C	T	90	23	NA	NA	MSK-T
B.18	17	<i>MAP2K4</i>	12016549	12016549	G	T	79	17	NA	NA	MSK-T
B.18	17	<i>NF1</i>	29665752	29665755	ACTT	-	131	42	NA	NA	MSK-T
B.2	14	<i>AKT1</i>	105246551	105246551	C	T	NA	NA	NA	NA	ddPCR
B.5	6	<i>ESR1</i>	152419923	152419923	A	G	NA	NA	NA	NA	ddPCR
B.20	6	<i>ESR1</i>	152419922	152419922	T	A	NA	NA	NA	NA	ddPCR
B.20	6	<i>ESR1</i>	152419926	152419926	A	G	NA	NA	NA	NA	ddPCR
B.9	6	<i>ESR1</i>	152419926	152419926	A	G	NA	NA	NA	NA	ddPCR
B.13	6	<i>ESR1</i>	152419926	152419926	A	G	NA	NA	NA	NA	ddPCR
B.6	14	<i>AKT1</i>	105246551	105246551	C	T	508	193	NA	NA	FMI
B.6	X	<i>ATRX</i>	76890117	76890117	C	A	986	99	NA	NA	FMI
B.6	16	<i>CBFB</i>	67063346	67063346	C	A	435	122	NA	NA	FMI
B.6	13	<i>IRS2</i>	110434520	110434520	A	G	732	293	NA	NA	FMI
B.6	1	<i>NOTCH2</i>	120464916	120464916	C	T	1025	492	NA	NA	FMI
B.6	17	<i>TP53</i>	7578526	7578526	C	A	625	56	NA	NA	FMI
B.6	17	<i>MAP2K4</i>	11958307	11958308	AT	-	902	235	NA	NA	FMI
G.56	12	<i>ARID2</i>	46244140	46244140	A	G	595	173	NA	NA	FMI
G.56	1	<i>IKBKE</i>	206653790	206653790	G	C	818	254	NA	NA	FMI
G.56	17	<i>TP53</i>	7578406	7578406	C	T	593	291	NA	NA	FMI
O.47	14	<i>AKT1</i>	105246551	105246551	C	T	325	162	NA	NA	FMI
O.47	X	<i>BCOR</i>	39923645	39923645	G	A	199	101	NA	NA	FMI
O.47	16	<i>CDH1</i>	68842748	68842748	C	G	255	38	NA	NA	FMI
O.47	22	<i>EP300</i>	41533754	41533754	G	A	349	38	NA	NA	FMI
O.47	17	<i>TP53</i>	7578391	7578391	T	-	263	42	NA	NA	FMI
O.51	14	<i>AKT1</i>	105246551	105246551	C	T	695	528	NA	NA	FMI
O.51	2	<i>ALK</i>	29446345	29446345	C	G	581	186	NA	NA	FMI
O.51	1	<i>ARID1A</i>	27106539	27106539	G	A	942	254	NA	NA	FMI
O.51	16	<i>CDH1</i>	68835596	68835596	C	T	552	293	NA	NA	FMI
O.51	20	<i>GNAS</i>	57429684	57429684	C	T	698	181	NA	NA	FMI
O.51	6	<i>IRF4</i>	394825	394825	G	C	797	199	NA	NA	FMI
O.51	9	<i>JAK2</i>	5022183	5022183	G	T	441	181	NA	NA	FMI
O.51	19	<i>NOTCH3</i>	15288741	15288741	C	T	278	86	NA	NA	FMI
O.51	5	<i>RICTOR</i>	38952489	38952489	T	C	762	381	NA	NA	FMI
O.51	19	<i>SMARCA</i>	11144536	11144536	C	G	537	188	NA	NA	FMI
		4									
O.51	17	<i>TP53</i>	7577082	7577082	C	G	584	274	NA	NA	FMI
O.51	16	<i>TSC2</i>	2124277	2124277	G	A	595	178	NA	NA	FMI
B.3	14	<i>AKT1</i>	105246551	105246551	C	T	379	250	NA	NA	FMI
B.3	5	<i>CSF1R</i>	149441339	149441339	G	A	459	321	NA	NA	FMI
B.3	7	<i>EGFR</i>	55270223	55270223	C	G	660	40	NA	NA	FMI
B.3	20	<i>GNAS</i>	57428395	57428395	G	C	542	163	NA	NA	FMI
B.3	17	<i>NF1</i>	29587463	29587463	A	C	642	199	NA	NA	FMI
O.42	14	<i>AKT1</i>	105246551	105246551	C	T	587	282	NA	NA	FMI
O.42	X	<i>ATRX</i>	76937995	76937995	G	A	1555	762	NA	NA	FMI
O.42	9	<i>FANCC</i>	97873869	97873869	C	A	806	322	NA	NA	FMI
O.42	17	<i>NF1</i>	29557336	29557336	C	T	669	274	NA	NA	FMI
G.35	14	<i>AKT1</i>	105246551	105246551	C	T	490	392	NA	NA	FMI
G.35	X	<i>AR</i>	66941751	66941751	C	G	950	408	NA	NA	FMI
G.35	X	<i>BCOR</i>	39921444	39921444	T	C	700	308	NA	NA	FMI
G.35	3	<i>CTNNB1</i>	41266104	41266104	G	T	1134	386	NA	NA	FMI

G.35	1	<i>MTOR</i>	11168338	11168338	C	A	806	596	NA	NA	FMI
G.35	16	<i>TSC2</i>	2135316	2135317	AA	GC	524	236	NA	NA	FMI
G.35	6	<i>ARID1B</i>	157099972	157099977	GCCCCG	-	547	170	NA	NA	FMI
					G						
G.35	1	<i>ARID1A</i>	27094459	27094460	-	ATA	856	531	NA	NA	FMI
G.35	4	<i>FBXW7</i>	153332912	153332913	-	GAG	1333	600	NA	NA	FMI
G.26	14	<i>AKT1</i>	105246551	105246551	C	T	824	758	NA	NA	FMI
G.26	12	<i>ARID2</i>	46246413	46246413	G	A	1480	740	NA	NA	FMI
G.26	17	<i>AURKB</i>	8108194	8108194	C	T	878	430	NA	NA	FMI
G.26	7	<i>CARD11</i>	2951813	2951813	G	T	958	450	NA	NA	FMI
G.26	1	<i>CDC73</i>	193117070	193117070	G	C	903	388	NA	NA	FMI
G.26	11	<i>MRE11A</i>	94180469	94180469	T	C	1410	677	NA	NA	FMI
G.26	1	<i>NOTCH2</i>	120468210	120468210	C	T	1215	644	NA	NA	FMI
G.26	1	<i>SPEN</i>	16203019	16203019	C	T	792	396	NA	NA	FMI
G.26	1	<i>ARID1A</i>	27024028	27024028	T	-	264	114	NA	NA	FMI
G.26	17	<i>TP53</i>	7577512	7577513	-	CAG	628	446	NA	NA	FMI
O.49	14	<i>AKT1</i>	105246551	105246551	C	T	481	120	NA	NA	FMI
O.49	6	<i>ESR1</i>	152420082	152420082	G	A	665	346	NA	NA	FMI
O.49	4	<i>FAT1</i>	187541438	187541438	C	T	934	458	NA	NA	FMI
O.49	15	<i>IGF1R</i>	99500400	99500400	C	T	1275	242	NA	NA	FMI
O.49	15	<i>NTRK3</i>	88678391	88678391	T	G	1145	103	NA	NA	FMI
O.49	7	<i>PIK3CG</i>	106508067	106508067	C	T	649	337	NA	NA	FMI
O.49	21	<i>RUNX1</i>	36252856	36252856	C	T	896	233	NA	NA	FMI
O.49	3	<i>SOX2</i>	181430992	181430992	G	A	904	172	NA	NA	FMI
O.49	1	<i>SPEN</i>	16235954	16235954	G	C	1008	202	NA	NA	FMI
O.49	20	<i>SRC</i>	36031599	36031599	C	A	753	361	NA	NA	FMI
O.49	X	<i>STAG2</i>	123191727	123191727	G	A	1189	250	NA	NA	FMI
O.49	X	<i>STAG2</i>	123215269	123215269	G	A	1148	207	NA	NA	FMI
O.39	4	<i>FAT1</i>	187540634	187540635	GT	AG	555	283	NA	NA	FMI
O.39	3	<i>PIK3CB</i>	138374293	138374293	C	T	413	29	NA	NA	FMI
O.39	10	<i>RET</i>	43615038	43615038	G	A	369	63	NA	NA	FMI
O.39	17	<i>RNF43</i>	56448310	56448310	G	A	383	126	NA	NA	FMI
O.39	3	<i>TGFBR2</i>	30713483	30713483	C	T	543	87	NA	NA	FMI
O.39	16	<i>CDH1</i>	68842392	68842403	ACAGA AGAGA GA	-	545	180	NA	NA	FMI
O.39	17	<i>SOX9</i>	70119752	70119753	CT	-	424	85	NA	NA	FMI
O.39	18	<i>SMAD4</i>	48584781	48584782	-	C	564	51	NA	NA	FMI
B.14	14	<i>AKT1</i>	105246551	105246551	C	T	458	380	NA	NA	FMI
B.14	15	<i>BLM</i>	91328232	91328232	C	T	1275	459	NA	NA	FMI
B.14	5	<i>MAP3K1</i>	56189379	56189379	C	T	1019	571	NA	NA	FMI
B.14	19	<i>PIK3R2</i>	18280070	18280070	C	T	488	244	NA	NA	FMI
B.14	6	<i>ARID1B</i>	157100056	157100070	AGGAG GAGCA GGAGC	-	314	122	NA	NA	FMI
B.14	5	<i>MAP3K1</i>	56168660	56168667	TGTCAA GT	-	1281	320	NA	NA	FMI
O.55	17	<i>TP53</i>	7578190	7578190	T	C	1086	337	NA	NA	FMI
O.55	7	<i>EGFR</i>	55242464	55242465	-	AATTCCC GTCGCTA TCAA	1957	411	NA	NA	FMI
O.55	10	<i>RET</i>	43572767	43572768	-	CGC	584	245	NA	NA	FMI
G.22	14	<i>AKT1</i>	105246551	105246551	C	T	325	166	NA	NA	FMI
G.22	3	<i>CTNNB1</i>	41266104	41266104	G	A	347	66	NA	NA	FMI

G.22	X	<i>MED12</i>	70339327	70339327	G	C	281	62	NA	NA	FMI
G.22	5	<i>RAD50</i>	131923769	131923769	C	T	318	80	NA	NA	FMI
G.58	14	<i>AKT1</i>	105243048	105243048	G	T	746	336	NA	NA	FMI
G.58	16	<i>CTCF</i>	67650737	67650737	G	A	557	434	NA	NA	FMI
G.58	3	<i>FOXL2</i>	138665163	138665163	G	C	629	258	NA	NA	FMI
G.58	5	<i>TERT</i>	1295228	1295228	G	A	101	44	NA	NA	FMI
G.58	4	<i>TET2</i>	106197552	106197552	C	T	1155	601	NA	NA	FMI
O.40	14	<i>AKT1</i>	105246551	105246551	C	T	540	119	NA	NA	FMI
O.40	6	<i>DAXX</i>	33287897	33287899	TTC	-	1669	417	NA	NA	FMI
O.36	4	<i>KIT</i>	55592100	55592100	A	G	662	331	NA	NA	FMI
O.36	13	<i>RB1</i>	48955394	48955394	C	T	509	173	NA	NA	FMI
O.36	18	<i>SMAD4</i>	48575159	48575159	C	T	543	11	NA	NA	FMI
O.36	17	<i>TP53</i>	7574021	7574021	C	A	468	234	NA	NA	FMI
G.23	14	<i>AKT1</i>	105246551	105246551	C	T	742	586	NA	NA	FMI
G.23	1	<i>ARID1A</i>	27056349	27056349	C	T	402	117	NA	NA	FMI
G.23	20	<i>ASXL1</i>	31023663	31023663	A	G	735	360	NA	NA	FMI
G.23	3	<i>ATR</i>	142281532	142281532	C	G	782	196	NA	NA	FMI
G.23	3	<i>CTNNB1</i>	41266113	41266113	C	T	829	240	NA	NA	FMI
G.23	7	<i>EGFR</i>	55270297	55270297	G	A	1013	608	NA	NA	FMI
G.23	6	<i>ESR1</i>	152419922	152419922	T	A	674	398	NA	NA	FMI
G.23	2	<i>MSH2</i>	47635615	47635615	G	A	814	309	NA	NA	FMI
G.23	13	<i>RB1</i>	49033844	49033844	C	T	656	387	NA	NA	FMI
G.23	17	<i>SOX9</i>	70119941	70119942	-	T	573	149	NA	NA	FMI
O.44	2	<i>ERBB4</i>	212566742	212566742	G	T	731	58	NA	NA	FMI
O.44	15	<i>IDH2</i>	90634818	90634818	C	T	517	57	NA	NA	FMI
O.44	15	<i>IGF1R</i>	99459984	99459984	G	T	582	303	NA	NA	FMI
O.44	14	<i>AKT1</i>	105246551	105246551	C	T	NA	NA	NA	NA	FMI
B.8	14	<i>AKT1</i>	105246551	105246551	C	T	NA	NA	NA	NA	FMI
O.52	14	<i>AKT1</i>	105246551	105246551	C	T	NA	NA	NA	NA	FMI
B.8	16	<i>CDH1</i>	68772218	68772218	C	T	NA	NA	NA	NA	FMI
O.52	16	<i>CDH1</i>	68862099	68862100	GT	-	NA	NA	NA	NA	FMI
O.44	20	<i>GNAS</i>	57429775	57429775	C	A	NA	NA	NA	NA	FMI
O.44	16	<i>GRIN2A</i>	9858211	9858211	T	C	NA	NA	NA	NA	FMI
O.44	15	<i>IDH2</i>	90634818	90634818	C	G	NA	NA	NA	NA	FMI
O.44	15	<i>IGF1R</i>	99459984	99459984	G	T	NA	NA	NA	NA	FMI
O.52	17	<i>MAP2K4</i>	NA	NA	NA	NA	NA	NA	NA	NA	FMI
B.8	17	<i>NF1</i>	29677279	29677279	C	A	NA	NA	NA	NA	FMI
O.52	3	<i>PIK3CA</i>	178936092	178936092	A	G	NA	NA	NA	NA	FMI
O.44	5	<i>RAD50</i>	131924537	131924537	C	G	NA	NA	NA	NA	FMI
B.8	12	<i>TBX3</i>	115110035	115110035	A	C	NA	NA	NA	NA	FMI
O.41	12	<i>KRAS</i>	25378562	25378562	C	T	112	3	NA	NA	MSK-cf

Chr, chromosome; Ref, reference; Alt, alternative; Data source is as defined in table S1.

Supplementary References

1. Al-Ahmadie HA, Iyer G, Lee BH, et al. Frequent somatic CDH1 loss-of-function mutations in plasmacytoid variant bladder cancer. *Nat Genet* 2016;48:356-8.
2. Cheng DT, Mitchell TN, Zehir A, et al. Memorial Sloan Kettering-Integrated Mutation Profiling of Actionable Cancer Targets (MSK-IMPACT): A Hybridization Capture-Based Next-Generation Sequencing Clinical Assay for Solid Tumor Molecular Oncology. *J Mol Diagn* 2015;17:251-64.
3. Frampton GM, Fichtenholtz A, Otto GA, et al. Development and validation of a clinical cancer genomic profiling test based on massively parallel DNA sequencing. *Nat Biotechnol* 2013;31:1023-31.
4. Lek M, Karczewski KJ, Minikel EV, et al. Analysis of protein-coding genetic variation in 60,706 humans. *Nature* 2016;536:285-91.
5. Chang MT, Asthana S, Gao SP, et al. Identifying recurrent mutations in cancer reveals widespread lineage diversity and mutational specificity. *Nat Biotechnol* 2016;34:155-63.
6. Shen R, Seshan VE. FACETS: allele-specific copy number and clonal heterogeneity analysis tool for high-throughput DNA sequencing. *Nucleic Acids Res* 2016;44:e131.
7. Greenman CD, Pleasance ED, Newman S, et al. Estimation of rearrangement phylogeny for cancer genomes. *Genome Res* 2012;22:346-61.